



OsBR6ox, a member in the brassinosteroid synthetic pathway facilitates degradation of pesticides in rice through a specific DNA demethylation mechanism



Yuxin Qiao^a, Li Ya Ma^{a,d}, Zhao Jie Chen^a, Yujue Wang^c, Yucheng Gu^b, Hong Yang^{a,*}

^a Jiangsu Key Laboratory of Pesticide Science, College of Sciences, Nanjing Agricultural University, Nanjing 210095, China

^b Syngenta Ltd, Jealott's Hill International Research Centre, Bracknell, Berkshire RG42 6EY, UK

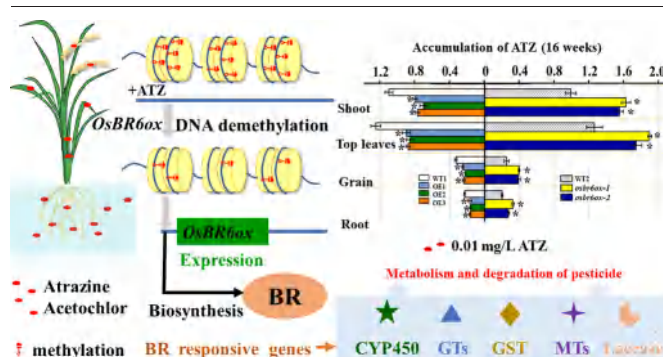
^c Syngenta Crop Protection AG, Rosentalstrasse 67, CH-4002 Basel, Switzerland

^d Institute of Agricultural Resources and Environment, Jiangsu Academy of Agricultural Sciences, Nanjing 210014, China

HIGHLIGHTS

- The content of BR and the rice growth were identified under ATZ/ACT stress.
- Transcription level of genes was related to pesticide detoxification.
- Lower accumulation of ATZ/ACT in rice by OsBR6ox modification
- Higher removal of ATZ/ACT from environment through rice overexpressing OsBR6ox
- A novel mechanism for the degradation of ATZ/ACT by DNA methylation-regulated p450

GRAPHICAL ABSTRACT



ARTICLE INFO

Editor: Jay Gan

Keywords:
Brassinosteroids
Atrazine
Acetochlor
Metabolism
Epigenetic modification

ABSTRACT

This manuscript described a comprehensive study on a pesticide degradation factor OsBR6ox that promoted the degradation of pesticides atrazine (ATZ) and acetochlor (ACT) in rice tissues and grains through an epigenetic mechanism. OsBR6ox was transcriptionally induced under ATZ and ACT stress. Genetic disruption of OsBR6ox increased rice sensitivity and led to more accumulation of ATZ and ACT, whereas transgenic rice overexpressing OsBR6ox lines (OEs) showed opposite effects with improved growth and lower ATZ and ACT accumulation in various tissues, including grains. OsBR6ox-mediated detoxification of ATZ and ACT was associated with the increased abundance of brassinolide (one of the brassinosteroids, BRs), a plant growth regulator for stress responses. Some Phase I-II reaction protein genes for pesticide detoxification such as genes encoding laccase, O-methyltransferase and glycosyltransferases were transcriptionally upregulated in OE lines under ATZ and ACT stress. HPLC-Q-TOF-MS/MS analysis revealed an enhanced ATZ/ACT metabolism in OE plants, which removed 1.21–1.49 fold ATZ and 1.31–1.44 fold ACT from the growth medium but accumulated only 83.1–87.1 % (shoot) and 71.7–84.1 % (root) of ATZ and 69.4–83.4 % of ACT of the wild-type. Importantly, an ATZ-responsive demethylated region in the upstream of OsBR6ox was detected. Such an epigenetic modification marker was responsible for the increased OsBR6ox expression and consequent detoxification of ATZ/ACT in rice and environment. Overall, this work uncovered a new model showing that plants utilize two mechanisms to co-regulate the detoxification and metabolism of pesticides in rice and provided a new approach for building up cleaner crops and eliminating residual pesticides in environments.

* Corresponding author at: Weigang No. 1, Chemistry Building, College of Sciences, Nanjing Agricultural University, Nanjing 210095, China.
E-mail address: hongyang@njau.edu.cn (H. Yang).

1. Introduction

Over the last decades, great efforts have been made to bio-remediate pesticide-contaminated soils (Besse-Hoggan et al., 2009; Jiang et al., 2019). One of the most prevalent approaches for dealing with the pesticides-contaminated soils is to increase the enzymatic activity in local soil microbial community to transform the chemicals into less or non-toxic metabolites (Sánchez-Trasviña et al., 2019). Although the promiscuous activities provided by microbes usually are a good start for detoxification, it is hard to figure out the evolutionary pathways for the metabolism of pesticides through an intermediate (Copley, 2009; Liu et al., 2020a). Unlike in bacteria, the majority of cellular absorbed drugs or xenobiotics are degraded through several canonical pathways in mammalian cells and similarly in plants (Scialli et al., 2014; Zhang and Yang, 2021). Both animals and plants have diverse and conservative genes following defined or currently undefined mechanisms to combat the influx of xenobiotics (Zhang et al., 2017).

Technically, understanding the insightful mechanisms for detoxification and specifics of pesticide metabolism in plants is also critical to developing engineered plants for bioremediation or cleaner healthy crops (Su et al., 2019; Ma et al., 2021). Currently, many catalytic processes for xenobiotics in plants like Phase I and II reactions such as hydroxylation, dealkylation or conjugation are well defined as the early stage of conversion, while Phase III or later stages as deep degradative metabolism through transport, compartmentation and mineralization remains elusive (An et al., 2017; Zhang and Yang, 2021). Interestingly, several plant signal molecules such as salicylic acid (SA) and jasmonic acid (JA) for defense responses have been recently reported to actively involve the pesticide metabolism and detoxification (Lu et al., 2015; Ma et al., 2018; Ma et al., 2021). The loss of function mutants with defective activities in rice phenylalanine ammonia lyase and isochorismate synthase for the biosynthesis of salicylic acid accumulated drastically higher levels of pesticide isoproturon with phytotoxic phenotypes, while administration of exogenous SA can restore the normal growth status of plants (Lu et al., 2020). Ma et al. (2021) functionally identified a rice F-box family member named COI1a (CORONATINE INSENSITIVE 1) to mediate atrazine degradation in plants through epigenetic demethylation of genomic DNA at CG context in the promoter region of COI1a. COI1a as a JA receptor was strongly induced by atrazine in rice. The atrazine-induced demethylated region in the COI1a promoter led to an enhancement of COI1a expression with an additional activity for atrazine degradative metabolism.

Brassinosteroids are a group of steroidal hormone-like molecules including castasterone (CS), brassinolide (BL), and 6-deoxocastasterone (6-DeoxoCS) in the BRs biosynthetic pathway (Yokota, 1999). BRs bind the receptor-like kinase BRI1 (brassinosteroid-insensitive 1) on the cellular surface through several biochemical events (e.g. autophosphorylation and dissociation of an inhibitory protein of BRI1 kinase Inhibitor 1) to activate the signal transduction cascades, leading to the changed expression of numerous genes and physiological consequences (Divi and Krishna, 2009). Recent review articles summarized the functional roles of BRs involved in plant growth, development and adaptation to environmental stress (Siddiqi and Husen, 2021; Zhang and Yang, 2021). Application of exogenous BRs increased plant resistance to pesticide toxicity by regulation of antioxidant system (Zhou et al., 2015; Sharma et al., 2018). In cucumber and grapevine, for example, pretreatment with the BRs variant 24-epibrassinolide alleviated the oxidant stress response caused by insecticides chlorpyrifos and chlorothalonil (Xia et al., 2009; Wang et al., 2017). Castasterone, one of the BRs, was reported to mitigate imidacloprid (pesticide)-responsive toxicity in Indian mustard (*Brassica juncea*) (Sharma et al., 2019). Even though BRs protect plants against pesticides, how BRs regulate the metabolic processes and enhance the detoxification is yet to be documented.

Atrazine (ATZ) and acetochlor (ACT) are two pesticides that have been used in large quantities worldwide over the last decades. Both chemicals are persistent in environments, and >0.01 mg/L ATZ residue was detected in groundwater (0.021 mg/L), surface streams (0.042 mg/L) and paddy soil (0.015–0.02 mg/kg) (Powell et al., 2011; Arora et al., 2014). In China,

acetochlor concentrations range from 0.03 to 709.37 µg/kg in riparian soils of Songhua River Basin, and 0.012–0.071 mg/kg in the farmland of northern regions (Sun et al., 2011). Investigation of ATZ/ACT uptake, accumulation, and degradation in plants can provide insights into bioremediation and development of ATZ/ACT resistant crops (Zhang and Yang, 2021). In this study, we found that both OsBR6ox transcription and BRs concentrations were significantly induced in rice exposed to ATZ or ACT. The processes were associated with the repressed DNA methylation at the CG context in the upstream of OsBR6ox. Overexpression of OsBR6ox in rice promoted plant detoxification, reduced accumulation of the pesticides, and facilitated the production of specific metabolites, whereas OsBR6ox knockout mutants displayed opposite effects. Expression of OsBR6ox promoted the Phase I and II metabolic reactions and the expression of corresponding pesticide degradation genes under ATZ and ACT stress. This is the first report on the functional characterization of OsBR6ox in mediating rice resistance to pesticides. The messages also signified a novel epigenetic mechanism (e.g. DNA methylation) that involves the signaling pathway of BRs in regulating the metabolism of xenobiotics in rice plants.

2. Materials and methods

2.1. Plant material, growth condition and treatment

Seeds of rice (*Oryza sativa*, Japonica) wild-types including Nipponbare (NP, WT1), Dong Jing (DJ, WT2), Kitaake (KT, WT3), and Hwayoung (HY, WT4), along with two independent *osbr6ox-1/2* T-DNA insertion lines (WT2) were sterilized and germinated at 28 °C. Two days later, germinating seedlings were transferred to the half-strength Hoagland solution and grown under simulated natural conditions for 10 days (Ma et al., 2019). The nutrient solution was changed every two days. Seedlings for acute experiments (six days) were exposed to 0.2 mg/L ATZ or ACT for analysis of physiological responses and accumulation of pesticides in rice tissues. The long-term (chronic) experiments were exposed to 0.01 mg/L ATZ or 0.02 mg/L ACT for 6–16 weeks. The ATZ and ACT concentrations of short-term exposure were below the real dosage of field application (ATZ, 22.3 kg/km²; ACT, 21.6 kg/km²), and the ATZ and ACT concentrations for long-term exposure were referred to the reports on the environmental residues.

2.2. Subcellular localization of OsBR6ox

The coding-sequence (CDS) of OsBR6ox was isolated from wild-type using the forward and reverse primers (Table S1). The amplified fragments were inserted into the pCambia1300-GFP vector under the control of a constitutive 35S CaMV promoter. The 35S::OsBR6ox-GFP fusion vector was transformed into leaf epidermis of tobacco (Khan et al., 2020). The GFP fluorescence signals were visualized on the confocal laser scanning microscopy and photographed (Confocal System-UltraView VOX, PerkinElmer).

2.3. Transcript analysis by qRT-PCR

The fresh tissues were harvested and frozen in liquid nitrogen. Total RNA was extracted using the Trizol following the instruction by the manufacturer (Monad Biotech Co., Suzhou) and treated with RNase-free DNase I (Takara). The RNA reverse transcription was performed using a TransGen kit (Biotech, Suzhou). The reaction mixture (20 µL) contained 1 µL of template cDNA, 10 µL of 2× TransScript Green q-PCR SuperMix, 8.2 µL RNase-free water and 0.4 µL primers (Table S1), with the following steps for reaction: one cycle of 94 °C for 30 s for denaturation, 40 cycles of 95 °C for 5 s and 60 °C for 30 s for annealing and extension (Lu et al., 2016a).

2.4. Preparation of OsBR6ox-overexpression lines

The full length of the OsBR6ox (LOC_Os03g40540) coding sequence was PCR-amplified using the specific primers (Table S1). The PCR product

was digested with BglII and SpeI (Table S1) and cloned into the corresponding sites of pCAMBIA1304 vector driven by a CaMV35S promoter (Liu et al., 2020b). The fusion vector was transformed by *Agrobacterium tumefaciens* into embryonic callus of rice. Thirty transgenic seedlings (T0) were built up. The initial transgenic generation was further cultivated and screened until homozygous lines (T3) were obtained. Three of overexpression (OE) lines were selected for subsequent functional identification.

2.5. Determination of growth and physiological responses to ATZ and ACT exposure

For chlorophyll determination, fresh leaf tissue (0.1 g) was collected, placed in a centrifuge tube containing 80 % acetone (pH 7.8), and stood under darkness for 24–36 h (Song et al., 2017). The mixture was centrifuged at 5000 g for 5 min. The supernatant was used for chlorophyll quantification. Chlorophyll were determined by reading the absorbance at 665 nm and 649 nm with a spectrophotometer, and calculated using the formula: chlorophyll content (mg/g FW) = $(6.10 \times OD_{665} + 20.04 \times OD_{649}) \times 5 / 0.1$.

The electrolyte permeability for cellular membrane damage was measured by placing fresh tissues in a tube with 20 mL deionized water. The sample stood at room temperature for 2.5 h and its solution was measured using an electrical conductivity meter with the reading as EC1. The conductivity of the killed tissues (EC2) was measured after boiling and cooling down to the room temperature. The electrolyte leakage was calculated as the ratio of $EC1/EC2 \times 100$ (Sun et al., 2021).

2.6. Analysis of McrBC-based DNA methylation and chromatin immunoprecipitation

The percentages of methylation at the CG, CHG and CHH contexts were estimated using the method of DNA bisulfate-sequencing technology (Lu et al., 2016a). Genomic DNA was isolated and digested by McrBC enzyme (methylation-dependent endonuclease). In parallel with it, a mock reaction was run at 37 °C for 16 h. The qRT-PCR was used to determine DNA methylation level. The level of methylation was inversely proportional to the ratio of McrBC/-McrBC. Histone methylation (H3K9me2) was measured by chromatin immunoprecipitation (ChIP) method (Feng et al., 2020). Samples were fragmented by sonication treatment and purification. The chromatin immunoprecipitation was tested using an assay Kit. The histone methylation level was analyzed by RT-PCR. Ubi10 and Actin1 were used for RT-PCR control. The amount of DNA immunoprecipitated by a Histone 3-specific antibody was applying to normalizing the relative abundance. Primer sequences were shown in Table S1.

2.7. Determination of ATZ and ACT accumulation in rice

Rice samples were harvested and pestled with liquid nitrogen. Five mL ultra-pure water and 10 mL acetonitrile were added to the sample, and the mixture was shaken. After 30 min, NaCl (2 g) was added and vibrated for 10 min. The extraction solution was centrifuged at 4000 g for 5 min. The upper acetonitrile phase (5.0 mL) with ATZ was concentrated to acetonitrile in a vacuum rotary evaporator (40 °C). The dried samples were dissolved and transferred to a 2 mL centrifuge tube with 30 mg graphitized carbon black and 50 mg primary-secondary amine, vortexed for 2 min, and centrifuged at 10,000 g for 3 min (Anastasiades et al., 2003). The supernatant was filtered through a 0.22 μm syringe membrane for analysis. For ACT, the upper acetonitrile phase was removed by evaporation (42 °C). The sample was mixed with a solvent (15:85 methanol:dichloromethane) and purified by a Florida Silica SPE column. The effluent was dried and dissolved in acetone (1 mL). The solution was through a 0.22 μm syringe membrane for analysis.

The ATZ analysis was performed by HPLC (Waters 515; Waters Technologies Co. Ltd.) equipped UV detector under the following conditions: Hypersil reverse phase C18 column (Thermo, 250 mm × 4.6 mm) was used for liquid chromatography separation under conditions; the mobile

phase, acetonitrile and water (35/65, V/V); rate, 0.8 mL/min; wavelength, 235 nm. The ACT analysis was performed by gas-chromatography (GC, System 7820A, Agilent) with an electron capture detector. An HP-5 capillary column (30 m × 0.320 mm, 0.25 mm internal diameter) was run with the oven temperature program as follows: 80 °C (starting temperature), increased to 210 °C at a rate of 40 °C/min, hold for 2 min at 210 °C, increased to 220 °C at a rate of 2 °C/min, once reached 220 °C, increased to 280 °C at a rate of 40 °C/min, and hold for 5 min at 280 °C. The total running time was 17.75 min. The carrier gas (Helium 99.999 % purity) was set at a flow rate of 0.8 mL/min. The injection sample volume was 1 μL without split. The spiked recovery of ATZ and ACT determination in rice tissues and nutrient solution was shown in Table S2.

2.8. Determination of ATZ and ACT metabolites and conjugates in rice

The extraction process of ATZ and ACT in rice was the same as Section 2.7. Unpurified extraction was concentrated and dissolved by 1 mL 50 % methanol. Samples were filtered and analyzed by UPLC-Q-TOF-MS/MS. The UPLC system (Shimadzu, Japan) equipped with a Poroshell 120 ECC18 (50 mm × 2.1 mm, 2.7 mm particle size, Agilent). The column temperature was 35 °C; the injection volume was 10 μL. The mobile phases A and B were ultrapure water with 0.1 % formic acid and acetonitrile, respectively. All the transformation products were characterized using Q-TOF-MS/MS (5600, AB Science, Redwood, CA, USA) with a positive electrospray ionization mode. The parameters are as following: ion spray voltage floating, 5500 V; temperature, 500 °C; ion source gas pressures, 50 psi; declustering potential, 80 V; collision energy, 35 eV; and collision energy spread, ± 15 eV. The mass spectrometer operates in a full scan TOF-MS mode with a 100–1000 m/z range and MS/MS (50–1000) mode (Ma et al., 2021).

2.9. In vivo determination of brassinosteroids in rice

The endogenous brassinolide (22R,23R,24S-2a,3a,22,23-tetrahydroxy-24-methyl-B-homo-7-oxa-5a-cholestan-6-one) was quantified using an Enzyme Linked Immunosorbent Assay (ELISA) Kit (Ruifan Biological Technology Co., Shanghai). Briefly, 50 μL of the sample extracted was added into the microwells pre-coated with brassinolide antibody, followed by addition of 100 μL horseradish peroxidase labeled detection antibody. The mixture was incubated at 37 °C for 60 min, and the substrate 3,3',5,5'-Tetramethylbenzidine was added. The sample was incubated at 37 °C for 15 min under darkness and measured at 450 nm.

2.10. Docking analysis

The three-dimensional conformations of ATZ and ACT were drawn using SYBYL 2.0 software (Shanghai Tri-I. Biotech. Inc., China). Molecular energy optimizations of three-dimensional conformations with a convergence criterion of 0.005 kcal/mol (Å) were obtained using conjugate gradient procedure, Tripos force field and Gasteiger-Huckel charge (Jiao et al., 2021). The crystal structure of OsBr6ox was downloaded from the RCSB (Research Collaboratory for Structural Bioinformatics) Protein Data Bank (PDB code 6a17, <https://www.rcsb.org/>). The ligand (9RL) was extracted and all H₂O molecules were removed from the structure. The obtained three-dimensional binding modes between ATZ and ACT compounds and 6a17 were determined using PyMol 1.7.6.

2.11. Statistical analysis

All experiments were independently performed at least in triplicate. For each replicate, >10 plants were used for analysis. One-way analysis of variance (ANOVA) was performed to determine the difference between treatments, and the significance was set at $p < 0.05$. All statistical analysis was carried out with SPSS (Version 22.0).

3. Results

3.1. OsBR6ox is located to chloroplasts and upregulated under ATZ and ACT stress

To clarify the subcellular localization of OsBR6ox, the OsBR6ox-GFP (green fluorescent protein) vector was constructed and expressed in tobacco leaves through *Agrobacterium tumefaciens* transfer protocol. The green fluorescence of OsBR6ox-GFP coincided with autofluorescence of chloroplast under the confocal microscopy, indicating that OsBR6ox resides in the chloroplast (Fig. S1A).

OsBR6ox was transcriptionally upregulated in ATZ-exposed roots and shoots. The significant expression occurred at 0.4–0.8 mg/L, with the shoot expression levels being 1.45–11.34 fold and those of root being 1.20–5.83 fold over the controls (Fig. S2A). A similar pattern of OsBR6ox expression was observed under ACT stress, in which the transcript levels were increased by 1.73–4.21 and 1.53–4.08 fold in shoots and roots, respectively (Fig. S2B).

3.2. Overexpression of OsBR6ox repressed ATZ and ACT toxicity in rice

To examine whether the expression of OsBR6ox could detoxify ATZ and ACT, transgenic rice overexpressing (OE) OsBR6ox was constructed. The qRT-PCR analysis showed that three OE lines had 12.5–33.9 fold higher transcripts than the wild-type (WT1) ($p < 0.05$) (Fig. S3). In the meantime, we took an advantage of two OsBR6ox-knockout mutants *osbr6ox-1* and *osbr6ox-2* with functional defects (Fig. S4). To ensure whether OsBR6ox

expression correlated with the abundance of endogenous products of BRs, the Enzyme-Linked Immunosorbent Assay (ELISA) was adopted to quantify the end product brassinolide catalyzed by OsBR6ox. There was a basal level of brassinolide without pesticides; upon exposure to the pesticides, the OE plants were found to accumulate more brassinolide, whereas the mutant lines accumulated less brassinolide in their shoots (Fig. 1) and roots (Fig. S5) than the wild-types, pointing out that the higher brassinolide concentration should be the result of OsBR6ox overexpression in OE lines.

We then performed a toxicological experiment using the transgenic materials. The OE and wild-type plants were exposed to 0.2 mg/L ATZ or ACT for six days. The growth response without ATZ and ACT was similar between the OE and WT1 plants (Fig. 2). When pesticides were administered, the OE rice showed better growth than WT1 in elongation and chlorophyll accumulation but low cell membrane permeability (Fig. 2; Fig. S6). The elongation of OE lines was increased by 53.1–62.5 % for shoot and 75.4–84.7 % for root compared to WT1. The increased expression of OsBR6ox was also beneficial to chlorophyll accumulation, with 1.14–1.33 (for ATZ) and 1.13–1.23 (ACT) fold over the WT1 control (Fig. 2D, I; Fig. S6). The OE lines had a weaker electrolyte leakage of biomembrane (or cell membrane permeability) than the WT1 (Fig. 2E, J; Fig. S6), suggesting that less cellular injury occurs in OE lines. The regulatory role of OsBR6ox was also proved by demonstrations of two independent dysfunction mutant lines *osbr6ox-1* and *osbr6ox-2*. In the presence of ATZ and ACT, both mutants showed a negative impact on plant fitness including the compromised plant growth and chlorophyll concentration and significantly increased electrolyte leakage (Figs. S7, S8). These results suggest that OsBR6ox is required for defense to the toxicity of the pesticides.

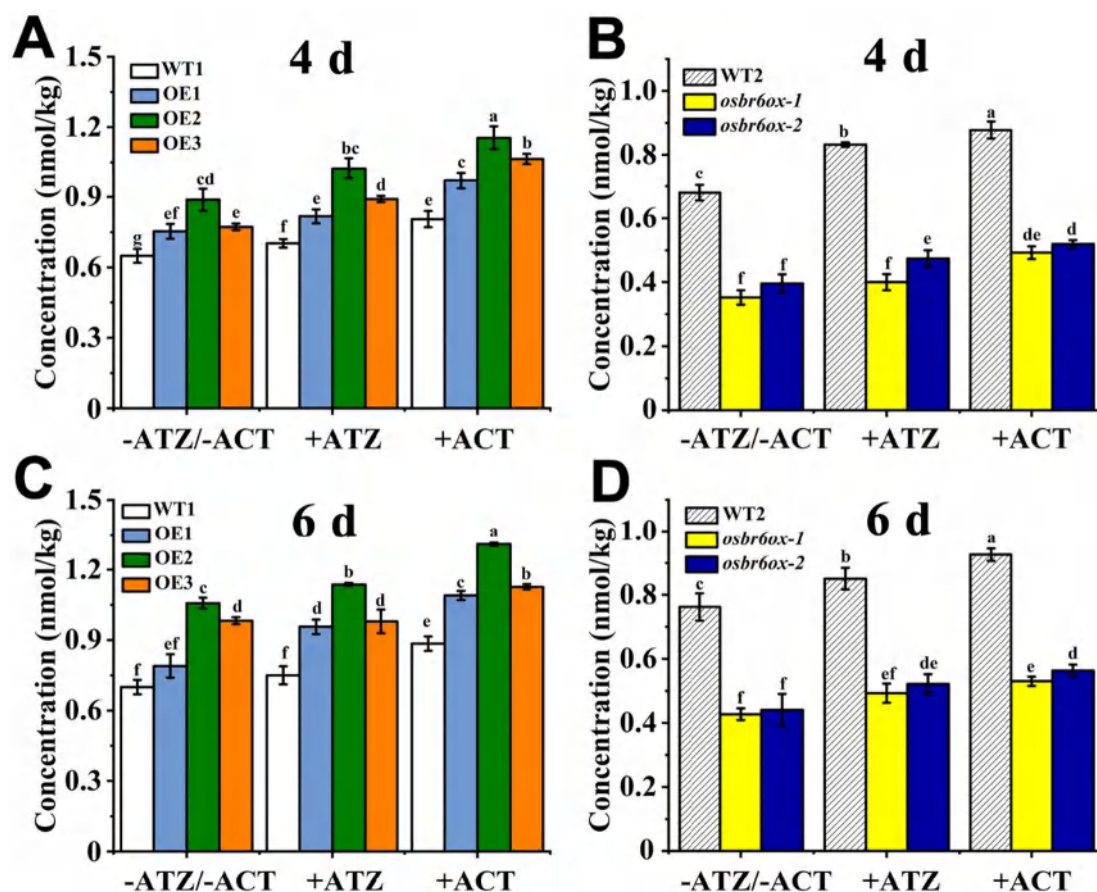


Fig. 1. Analysis of brassinolide generation in the shoots of OE lines, mutants and their corresponding wild-types (WT1: NP, WT2: DJ) under ATZ and ACT stress by ELISA. Ten day-old rice was treated with 0 (-ATZ/-ACT) and 0.2 mg/L ATZ or ACT for 4 d and 6 d. (A, C): The brassinolide concentrations in the OE lines and wild-type were measured after treatments for 4 d (A) and 6 d (C). (B, D): The brassinolide concentrations in the mutants and wild-type were measured after treatments for 4 d (B) and 6 d (D). Values are the means \pm SD ($n = 3$). Means followed by different letters are significantly different between the genotypes of plants ($p < 0.05$, ANOVA).

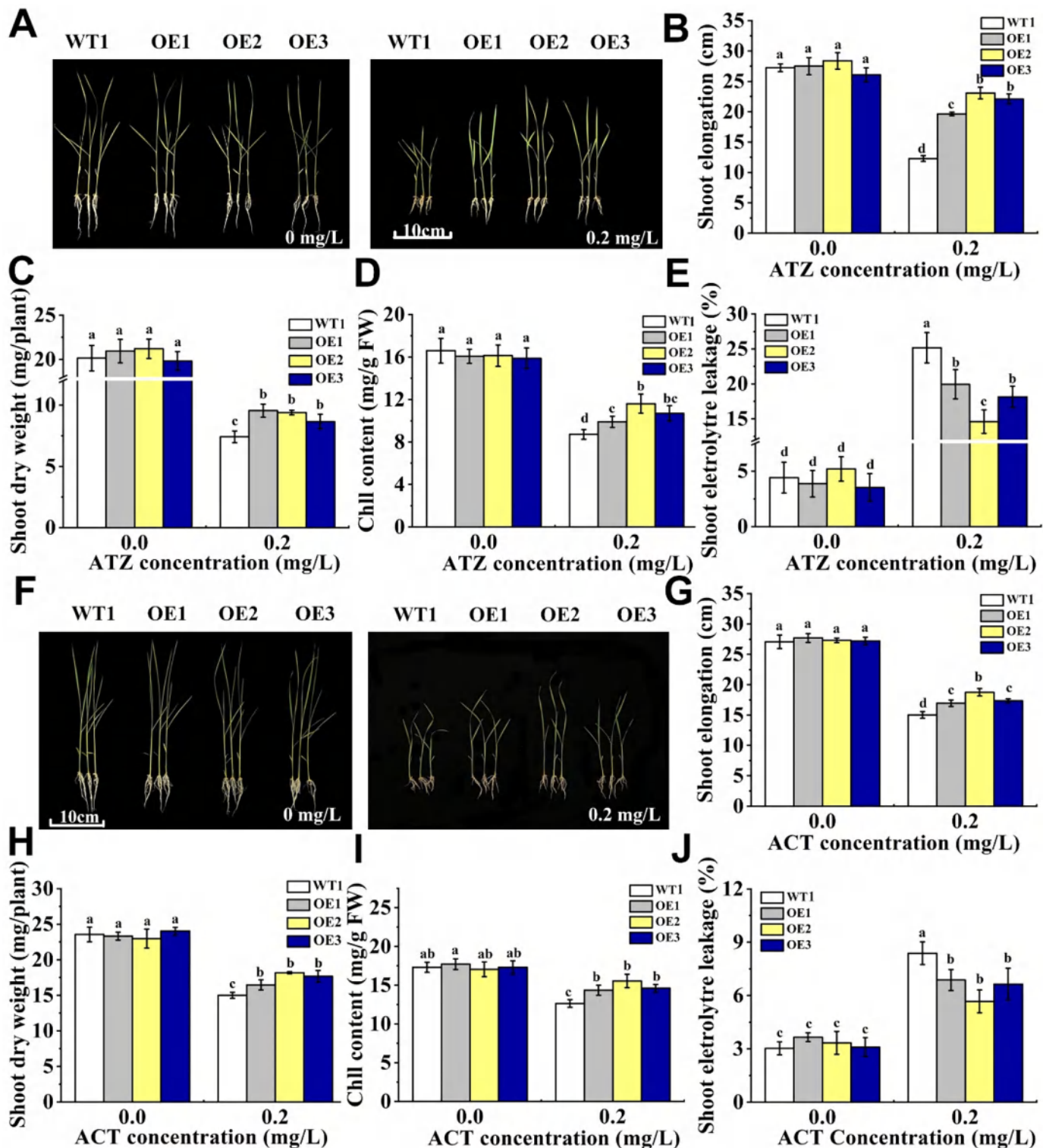


Fig. 2. Growth analysis of shoots in OE lines and wild-type (WT: Nipponbare) under ATZ and ACP exposure. Ten-day-old rice plants were exposed to ATZ (0.2 mg/L) and ACT (0.2 mg/L) for 6 d. (A): Phenotypes of WT and OE lines. (B, G): Elongation of shoots. (C, H): Dry mass of shoots. (D, I): Chlorophyll content. (E, J): Membrane permeability of shoots. Values are the means \pm SD (n = 3). Means followed by different letters are significantly different within each biotype or treatment (p < 0.05, ANOVA).

3.3. Overexpression of OsBR6ox reduced ATZ and ACT accumulation in rice

A short-term experiment with 0.2 mg/L ATZ and ACT exposure for six days was conducted to examine the removal of the pesticides by rice from its growth environment and plants. The OE plants removed more ATZ and ACT from rice growth medium and accumulated less ATZ and ACT in

plant tissues compared to WT (Fig. 3; Fig. S9). Meanwhile, both *osbr6ox-1* and *osbr6ox-2* mutant plants displayed an opposed effect (Fig. 3; Fig. S9). A long-term experiment (up to 16 weeks) with realistic environmental concentrations of the pesticides was further performed. Both OE and mutant plants were grown on the nutrient solution containing 0.01 mg/L ATZ or 0.02 mg/L ACT. Maturity plants were sampled at their stages of vegetative

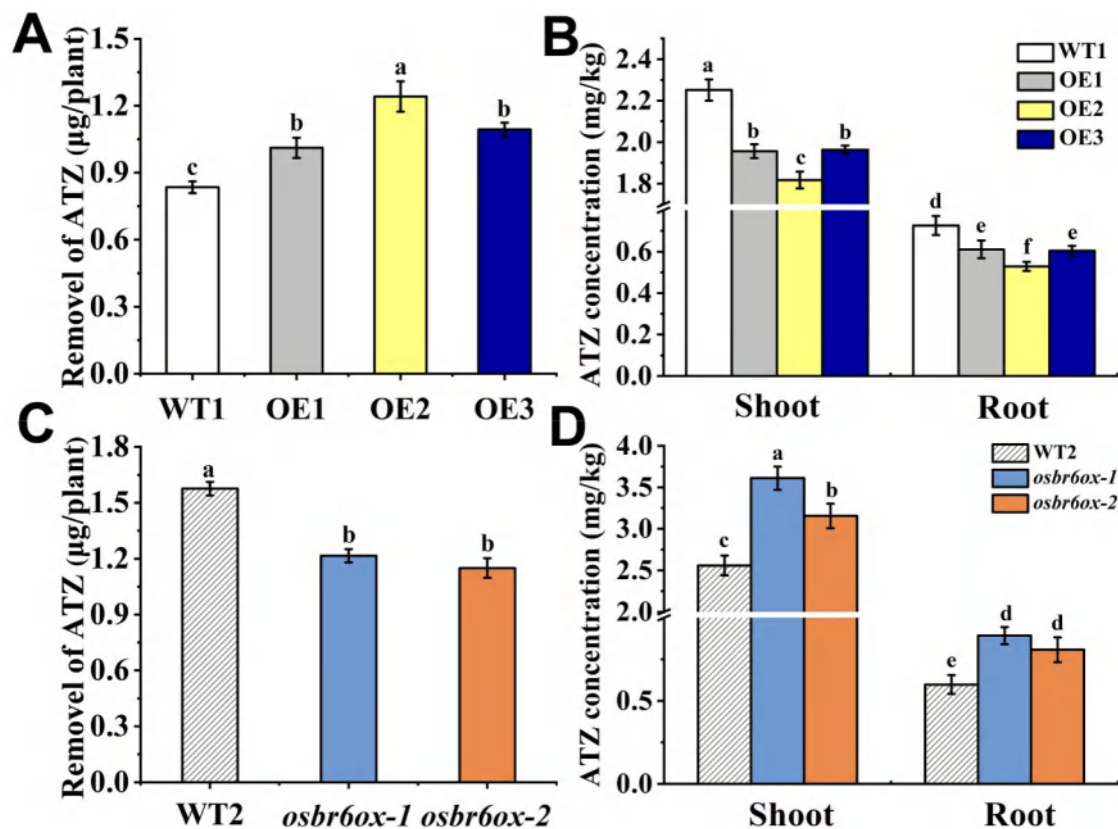


Fig. 3. Short-term experiment with ATZ removal from growth medium and accumulation in OE, mutant lines and wild-types (WT1: Nipponbare; WT2: DJ). (A, C): Ten day-old rice plants were treated with 0.2 mg/L ATZ for 2 d and the removal of ATZ from growth media by the plants were measured. (B, D): Ten day-old rice plants were treated with 0.2 mg/L ATZ for 6 and ATZ accumulation in plants were measured. Values are the means \pm SD (n = 3). Means followed by different letters are significantly different between the genotypes of plants ($p < 0.05$, ANOVA).

(6 weeks), heading (12 weeks), filling (14 weeks) or maturity (16 weeks), respectively. Overall, all OE lines accumulated lower levels of ATZ (Fig. 4) and ACT (Fig. S10) than the WT and mutant lines. Notably, the ATZ and ACT concentrations in the ripening grains in OE plants were constantly much lower than the wild-types (Fig. 4; Fig. S10C). The concentrations of ATZ in OE lines were reduced by 24.2–33.3 % and those of ACT in OE lines were decreased by 22.5–37.3 % compared to the wild-type controls. On the other hand, the mutant plants had a higher level of ATZ and ACT (Fig. 4; Fig. S10). These results suggest that OsBR6ox can play a primary role in reducing the pesticides in rice plants.

3.4. Overexpression of OsBR6ox promoted expression of major genes in Phase I and II

To investigate whether OsBR6ox was able to promote the expression of genes related to pesticide degradation, we selected six Phased I and II protein genes including two CYPs (CYP74A2, CYP88A5) (Tan et al., 2015), laccase (Huang et al., 2016), O-methyltransferase (Lu et al., 2016b), glutathione S-transferase (Zhang et al., 2016) and glycosyltransferase (GT) (Zhang et al., 2017) for qRT-PCR analysis. Following exposure to 0.2 mg/L ATZ or ACT for six days, all tested genes were upregulated in the shoots of OE lines, whereas the genes were downregulated in the knock-out mutant although their expression varied differently (Fig. 5). These results suggest that expression of OsBR6ox can confer detoxification and metabolism of ATZ and ACT through its downstream degradative enzymes.

3.5. Overexpression of OsBR6ox generated more ATZ and ACT metabolites

The metabolites of OE line, mutants and their corresponding wild-types (WT1 and WT2) were characterized by UPLC-Q-TOF-MS/MS. The key

factors for characterization, retention time and degradation products were illustrated (Table S3–4). The extracted ion chromatograms of ATZ and ACT metabolites and conjugates in rice were shown in Fig. S11, S12. Nine metabolites and ten conjugates of ATZ were detected (Fig. 6A, Figs. S13, S14). We also successfully characterized 12 metabolites and 11 conjugates in rice exposed to ACT (Fig. 6B, Figs. S15, S16).

Further quantitative analysis on the metabolites revealed that compared to the wild-type, the relative contents of metabolites of both ATZ and ACT in the OE plants were significantly higher, while those in the mutant lines were lower (Fig. 7). For ATZ, more metabolites were found in rice shoots than roots; and the additional metabolites in shoots were those m/z 228 and three conjugates m/z 315, m/z 343, and m/z 430 (Fig. 7A–D). In shoots, the concentrations of dominant metabolites m/z 230 and m/z 214 in OE lines were 1.14 and 1.70 times larger than those in the wild type, whereas the concentrations of the two metabolites in the mutants were lower (0.24 and 0.13 times lower than the ones in the wild type). With regards to the conjugates created by Phase II reaction, the cysteine (m/z 301) and glutathione (m/z 487) conjugates also displayed higher levels in OE plants, with 1.16 and 1.23 times over the wild type. Additional conjugates in the OE lines were detected (Fig. 7B). As for ACT, the contrasting changes in metabolites or compounds between the OE and mutant plants were detected (Fig. 7).

3.6. Molecular docking study on interaction of OsBR6ox and ATZ/ACT

Using the amino acid sequence of OsBR6ox as a template, three-dimensional structures of CYP90B1 (PDB:6a17) was selected for homology modeling, and ATZ and ACT were molecularly docked with OsBR6ox (Fig. 8). ATZ was embedded in the active pocket of OsBR6ox protein via connection of hydrogen-bonding and hydrophobic interactions with some

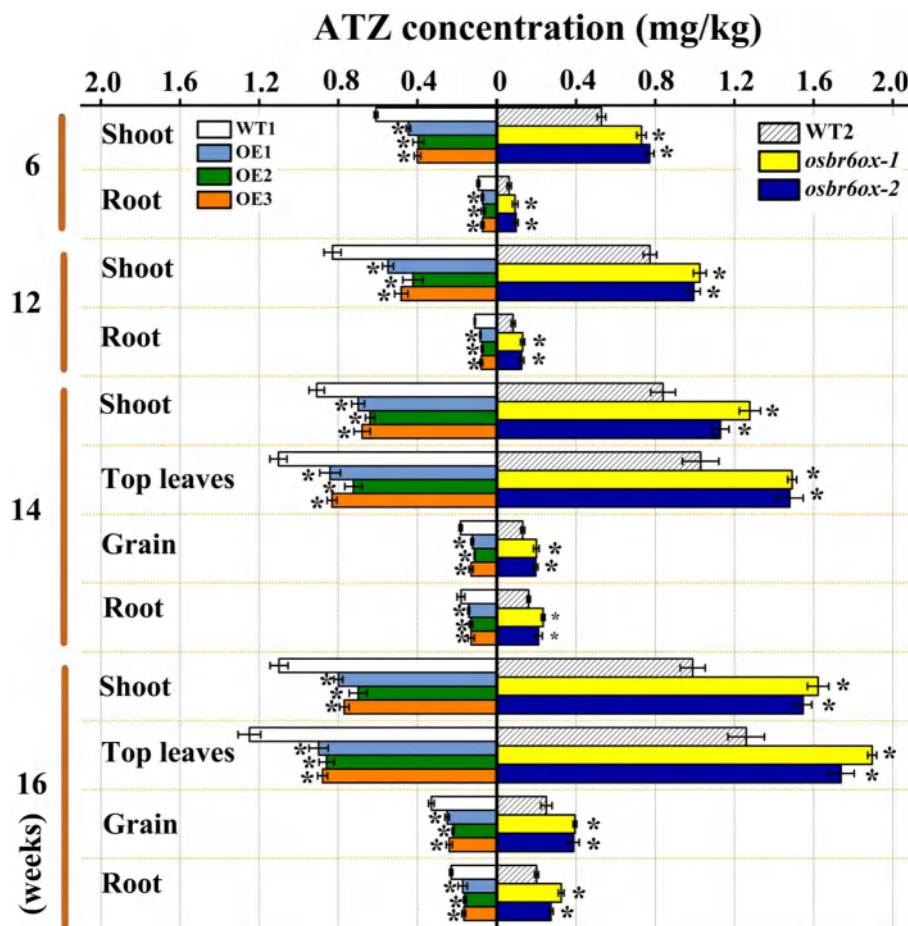


Fig. 4. Long-lasting experiment with ATZ accumulation in OE, mutant lines and WTs. Ten day-old rice seedlings were exposed to 0.01 mg/L ATZ for 6, 12, 14, and 16 weeks (lifespan). Different tissues were harvested and ATZ concentrations were measured. Values are the means \pm SD ($n = 3$). Means followed by different letters are significantly different between genotypes ($p < 0.05$, ANOVA).

crucial amino acid residues including those of tyrosine at 280 position (TYR 280), threonine at 285 position (THR 285), tyrosine at 101 position (TYR 102), arginine at 455 position (ARG455), and alanine at 106 position (ALA 106) (Fig. 8). The hydrogen bonds were formed by ARG 455 and TYR 102 with the nitrogen atom on the ATZ triazine ring and side chain amino group. The residues TYR 280, THR 285, and ALA 106 were similarly critical in a continuous belt of hydrophobic interactions encircling the carbon atom on the side chain of ATZ. ACT had a hydrophobic interaction with amino acid residues including residues methionine at position 125 (MET 125), valine at position 381 (VAL 381), and alanine at position 311 (ALA 311). In addition, residue serine at position 307 (SER 307) formed a halogen bond with the chlorine atom on ACT. Systematic analysis of the crystal structure in PDB revealed that the interaction between the halogenated ligand and target protein is the basis of many biomolecular interactions (Taylor, 2017). Based on the results, OsBR6ox would likely work in this way of targeting ATZ and ACT residues.

3.7. Expression of OsBR6ox was promoted by demethylation in the upstream of the gene

During the investigation, we found that in the promoter region (R1) upstream of OsBR6ox, there is a specific fragment (-446 to -353) where the CG and CHG methylation is dynamically changed in the absence or presence of ATZ (Fig. S17A). With ATZ, the total methylation level in this region decreased by 39.8 %, and the methylation at CG and CHG (H: A, C, T or G) declined by 52.1 % and 23.5 %, respectively (Fig. S17A). To clarify whether or not ATZ-induced DNA demethylation was associated with

OsBR6ox expression, a couple of mutant lines lacking DNA methylation activities come into application. DNA methylation levels in the Osmet1–2 and Osmet1–2 lines (mutation at CG) were significantly lower compared to the wild-type control (Fig. S17B). Since the CG methylation at cytosine was linked to the histone H3K9me2 marker catalyzed OsSDG714 in the chromatin (Ding et al., 2007), the H3K9me2 level in the upstream of OsBR6ox was examined in the Osdsg714 mutant using a specific H3K9me2 antibody depending on the chromatin immunoprecipitation technique. The H3K9me2 marks were also reduced in the R1 of OsBR6ox, whose level was only 81.4 % of the control, and yet, such specific marks at R2 and R3 remained unchanged (Fig. S17). Furthermore, the OsBR6ox expression was measured in a DNA demethyltransferase mutant called Osros1. There was a negative connection between the OsBR6ox methylation and transcription (Fig. S17), indicating that hypermethylation of OsBR6ox in rice would repress OsBR6ox transcription. These results signified that the expression of OsBR6ox was dynamically regulated by DNA methylation in the presence of ATZ.

4. Discussion

This study demonstrated the comprehensive identification of a new function of OsBR6ox as a major regulator in the BR synthetic pathway that displayed active participation in detoxification and metabolism of the pesticides ATZ and ACT. OsBR6ox overexpression was found to generate more brassinolide, whereas knocking out OsBR6ox drastically lowered brassinolide accumulation in rice. Intriguingly, identifying an ATZ-exposed methylome revealed a specific region in the OsBR6ox promoter

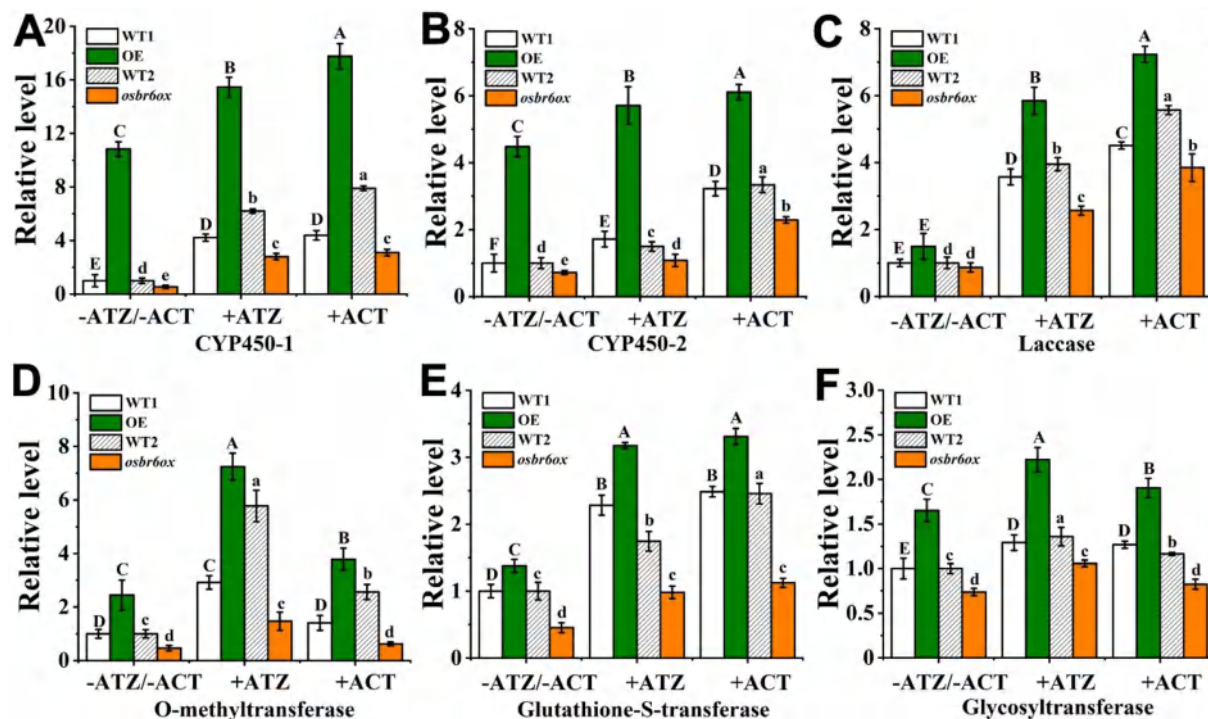


Fig. 5. Analysis of transcriptional expression of defense genes in the shoots of OE-2, *osbr6ox*-1 and their corresponding wild-types (WT1: NP, WT2: DJ) under ATZ and ACT stress by quantitative RT-PCR. Ten-day-old rice plants were exposed to 0 (-ATZ/-ACT) and 0.2 mg/L ATZ or ACT for 6 days. Defense-related genes including CYP74A2 (LOC_Os03g12500) (A), CYP88A5 (LOC_Os06g02019) (B), laccase (LOC_Os12g15680) (C), O-methyltransferase (LOC_Os04g09604) (D), glycosyltransferase (LOC_Os04g40520) (E) and glutathione-S-transferase (LOC_Os10g38489) (F). Values are the means \pm SD. Means followed by different letters are significantly different between the genotypes of plants, upper and lower case letters are used to distinguish different wild-types ($p < 0.05$).

region with a significantly lower DNA methylation at CpG context and histone H3K9me2 marks associated with the enhanced transcription of *OsBR6ox*. This finding represents a new layer of how the pesticides broke down through the plant biosystems with a complex mechanism of rice plants to adapt to their environments. This is the first instance so far reported.

BRs respond to a variety of internal and external factors (Siddiqi and Husen, 2021). Several studies focus on the impact of its external supply on pesticide detoxification in plants (Sharma et al., 2018). Treatment with 24-epibrassinolide, a component in the BRs synthetic pathway of plants like tomatoes, cucumbers, strawberries, and mustard attenuated toxic symptoms and conferred less accumulation of pesticides (organophosphorus, organochlorine and carbamate) (Xia et al., 2009; Zhou et al., 2015; Wang et al., 2017; Sharma et al., 2019). Such resistant responses following BRs treatment were associated with a lower degree of oxidative stress due to the promoted expression of antioxidants and other degradative enzymes such as superoxide dismutase (SOD), peroxidase (POD), catalase (CAT), respiratory burst oxidase (RBOH) and CYP450 (Zhou et al., 2015; Sharma et al., 2019). However, the upstream regulatory mechanisms underlying the detoxification of pesticides are not understood, and the biological processes of pesticide metabolism and degradation remain elusive.

The molecular structures of ATZ and ACT are different, but rice plants seemingly had similar biochemical metabolisms for physiological responses upon exposure to the pesticides. *OsBR6ox* overexpression improved the growth and resistance to ATZ and ACT, which should be attributed to the enhanced generation of endogenous BRs in rice (Fig. 1; Fig. S5). This confirmed that *OsBR6ox*-regulated detoxification of ATZ and ACT in rice was at least partially through the BRs signaling pathway. External BRs-promoted resistance to pesticides was associated with upregulation of some Phase I reaction enzymatic genes such as GSTs (Glutathione S-transferases) and CYP450s (Sharma et al., 2017; Wang et al., 2017). However, whether these genes specifically regulate the metabolism and

degradation of pesticides requires functional validation. To address the question, we analyzed the transcripts of some canonical phased reaction genes whose functions have been well characterized. We found that all selected genes encoding CYP74A2, CYP88A5, laccase, O-methyltransferase, glycosyltransferase and GST in OE plants were transcriptionally upregulated under ATZ and ACT exposure (Fig. 5) (Tan et al., 2015; Huang et al., 2016; Lu et al., 2016b; Zhang et al., 2016; Zhang et al., 2017), suggesting that they were most likely involved in the BRs-mediated metabolism and degradation pathway.

To bridge the gap between the Phase I enzymes and their catalyzed metabolites, we characterized a total of nine ATZ and twelve acetochlor metabolites (in Phase I) by UPLC-Q-TOF-MS/MS. Amongst the metabolites, the ATZ dehydrogenation product (DHA) and a variety of ATZ dealkylated metabolites (DACT, DEA, DMA, and DIA) were identified to link the function of CYP450s (Tan et al., 2015; Zhang and Yang, 2021). Notably, the metabolic product DACT was identified for the first time in rice and most likely associated with the function of CYP450 in ATZ dealkylation. Another ATZ metabolite hydroxyatrazine (HA) was identified (Fig. S13). These identified metabolites usually do not pose an environmental risk. For example, Scialli et al. (2014) reported that HA fails to affect the rat or rabbit embryo-fetal development even though the dosage comes up with the level of producing maternal toxicity; Tai et al. (2021) concluded that ATZ degradation products DIA and DACT have no potential risks to zebrafish hatchability, somite formation, heart, and embryo under environmentally realistic concentrations. Laccase is a unique kind of multi-copper containing oxidase, playing important roles in molecular modification and detoxification by catalyzing the oxidation of multi-substrates (Sánchez-Trasviña et al., 2019). Our previous demonstration pointed out that ectopic expression of a rice laccase gene conferred yeast (*Saccharomyces cerevisiae*) tolerance to ATZ by accumulation of deaminated and hydroxylated ATZ (HDHA) (Huang et al., 2016). The present study characterized an HDHA precursor HEA without deamination, suggesting that laccase may be also engaged in the ATZ degradative process in rice.

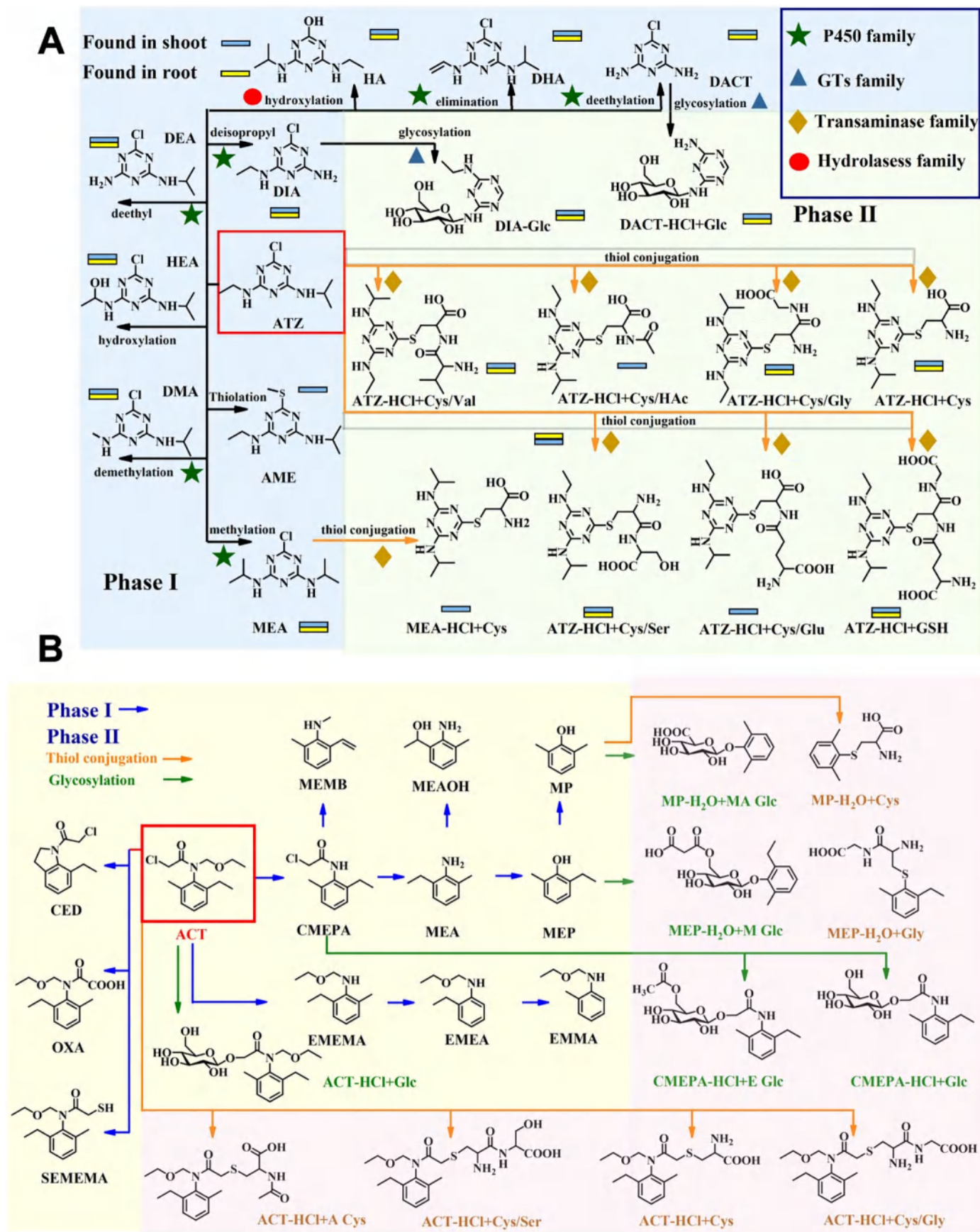


Fig. 6. Proposed metabolic pathways of ATZ and ACT pesticides. (A): ATZ and (B): ACT in shoots and roots of rice. The metabolites and conjugates of ATZ and ACT were characterized using HPLC/Q-TOF-MS/MS.

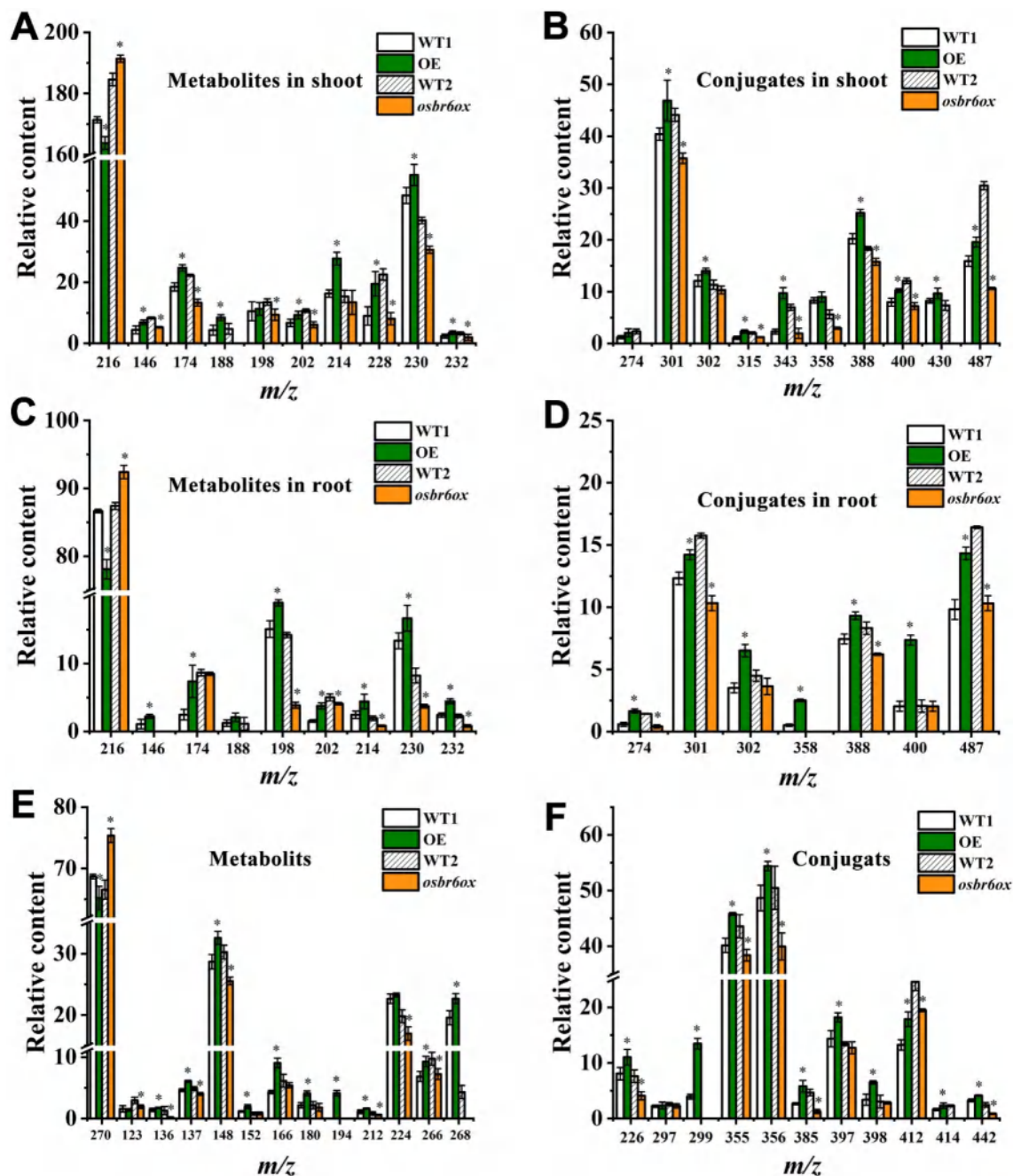


Fig. 7. Relative contents of ATZ and ACT metabolites and conjugates in WT (WT1, WT2), OE lines and mutants. Relative contents of ATZ metabolites in shoots (A) and roots (B). Relative contents of ATZ conjugates in shoots (C) and roots (D). Relative contents of ACT metabolites (E) and conjugates (F) in rice tissues. Ten-day-old rice seedlings were exposed to 0.2 mg/L ATZ for 6 days. Values are the means \pm SD ($n = 3$). Asterisks indicate significant differences between WT, OE line and mutant ($p < 0.05$).

Of the twelve metabolites of ACT, metabolites CMEPA, MEA and MEAOH could be produced by highly conserved human CYP450 isoforms CYP3A4 and CYP2B6 (Coleman et al., 2000). Transgenic Arabidopsis by chloroplast transformation expressing an acetochlor-degradative N-dealkylase gene named CndA (from a bacterium *Sphingomonas wittichii* DC-6) also showed an ACT-resistant phenotype manifested by a significant reduction of its residues including CMEPA in soil and water (Chu et al., 2020). In this study, more ACT metabolites were identified with smaller molecules and simpler structures such as MEP and MP. The metabolites were derived from CMEPA through dealkylation, hydroxylation or other metabolic reactions, which were most likely catalyzed by a CYP450 in the BRs pathway.

In Phase II reaction, ten ATZ conjugates were identified including two glycosylation and eight amino acid derivatives. Many glycosyltransferases in plants actively glycosylate their targets such as secondary metabolites and artificial herbicides to make them detoxified by modifying their polarity (Li and Yang, 2013; Zhang et al., 2017). We identified a compound that binds DACT to a glucose (DACT-HCl + Glc), and its formation was likely relevant to the upregulated expression of the glycosyltransferase. There was another glyco-conjugate metabolite DIA + Glc, which was consistent with the previously reported compound in rice (Zhang et al., 2017). The combination of DACT and DIA with glucoses was implied that ATZ was easier to establish active sites to bind to glucose after CYP450-catalyzed dealkylation.

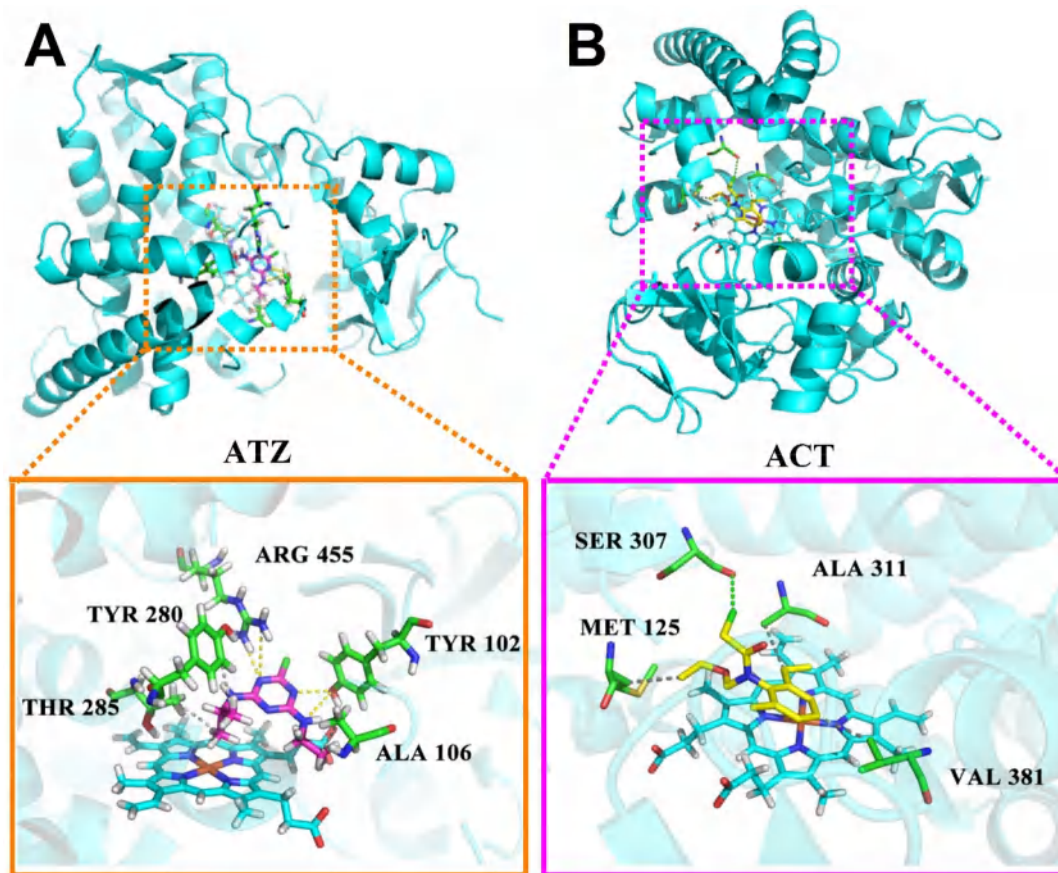


Fig. 8. The receptor-ligand interaction of ATZ (A, C) and ACT (B, D) with the BR6ox active site using PyMol soft from molecular docking.

There was another important pathway linking the metabolism of amino acid to ATZ, by which some types of thiol compounds were synthesized to diminish ATZ-induced reactive oxygen species (ROS) (Adil et al., 2020). Most of the low molecular weight thiol compounds originate from glutathione and cysteine (Pivato et al., 2014). GSTs promote glutathione to conjugate a variety of substrates including herbicides for detoxification (Dixon et al., 1998). We detected a conjugate (ATZ-HCl + GSH) and cysteine or cysteine-containing dipeptide conjugates such as ATZ-HCl + Cys and ATZ-HCl + Cys/Gly. Further analysis found that the amino acid conjugates ATZ-HCl + GSH and ATZ-HCl + Cys. The glucose conjugate DIA + Glc had higher abundance in the overexpression rice, which allowed us to assume the contribution of GST and GTs promoted by BRs under ATZ stress.

The eleven ACT conjugates identified comprised five glucose conjugates and six amino acid conjugates. Apart from ACT-HCl + Glc, four glucose conjugates (MEP-H₂O + M Glc, MP-H₂O + MA Glc, CMEPA-HCl + Glc, and CMEPA-HCl + E Glc) came from dealkylated ACT and glucose combinations. These results confirmed our speculation that BRs-induced upregulation of CYP450s would make it easier to bind glucose to pesticides by forming an active site after dealkylation. As amounts of all ACT conjugates in OE rice exceeded those of wild type, it confirms that OsBR6ox overexpression can promote the metabolism and degradation of ACT.

The genomic DNA methylation typically occurring at CG, CHG, and CHH sites is an important epigenetic mechanism for gene expression, crop domestication and adaptation to environmental stress (Feng et al., 2021; Ma et al., 2021). Up to date, only limited knowledge is available on the epigenetic mechanisms for detoxification and accumulation of pesticides like atrazine in plants (Scarpato et al., 2020; Zhang and Yang, 2021). Previous studies showed that DNA methylation is sensitive to environmental pesticide residues (Lu et al., 2016a; Wirbisky-Hershberger et al., 2017; Ma et al., 2019). In the current study, a dynamic change in methylation/demethylation at the specific region of OsBR6ox promoter

by ATZ stress was identified. This reaction was also observed in a recent study on zebrafish larvae (Wirbisky-Hershberger et al., 2017), where they reported a reduced expression of DNMTs (DNA methylases) after atrazine treatment and consequently led to a lower level of DNA methylation.

To dissect where ATZ-induced DNA demethylation in OsBR6ox is able to alter the gene expression and contribute to phenotypic resistance to ATZ toxicity, several mutants defective in DNA methylation activity were assessed (Feng et al., 2020; Ma et al., 2019). ATZ-mediated demethylation in the specific region (R1) of OsBR6ox was found to be associated with increased expression of OsBR6ox (Fig. S17). Furthermore, the ATZ-induced OsBR6ox demethylation was also detected in OsSDG714 mutant, because loss of the gene (OsSDG714) function led to a lower level of histone H3K9me2 marks, pointing out that the reduced DNA methylation in the upstream of OsBR6ox is closely related to its surrounding histone demethylation. Overall, the upregulation of OsBR6ox expression by the epigenetic mechanism through DNA and histone demethylation should be responsible for the BRs signal transduction pathway for degradation of the pesticides.

5. Conclusions

This study demonstrated that rice exposure to ATZ and ACT increased the transcriptional expression of OsBR6ox by triggering DNA demethylation mainly at CpG context in the promoter region of OsBR6ox. The functional role in detoxifying ATZ and ACT played by OsBR6ox is most likely through the BRs signal molecules which in turn promoted the expression of Phase I and II reaction components responsible for the metabolism and detoxification of the pesticides. Our study illustrated a new layer of regulatory mechanisms for pesticide dissipation through the BRs signaling pathway with a detoxic function to regulate plant adaptation to xenobiotic-polluted environments, and also provide a model for biological engineering of plants or crops to facilitate the complete mineralization of pesticides

residues. Further investigation will focus on the genetic connection between OsBR6ox and its downstream enzymes involved in the metabolism of pesticides in rice plants.

CRedit authorship contribution statement

Yuxin Qiao, undertook the molecular, genetic and physiological experiments, analyzed metabolites and degraded products. Li Ya Ma, carried out experiments with ATZ/ACT characterization in plants. Zhaojie Chen, carried out the plant growth experiments. Yuejue Wang and Yucheng Gu carried out the language modification. Hong Yang, conceived and designed the study; drafted, modified and finally proof-edited the manuscript.

Declaration of competing interest

The authors declare that they have no known competing financial interests or personal relationships that could have appeared to influence the work reported in this paper.

Acknowledgements

The authors acknowledge the financial support of the National Natural Science Foundation of China (No. 21976092), the Postgraduate Research & Practice Innovation Program of Jiangsu Province (KYCX21_0562) and the Syngenta Ph.D. Fellowship Programme.

Appendix A. Supplementary data

Supplementary data to this article can be found online at <https://doi.org/10.1016/j.scitotenv.2022.156503>.

References

- Adil, M.F., Sehar, S., Han, Z.G., Lwalaba, J.L.W., Jilani, G., Zeng, F.R., Chen, Z.H., Shamsi, I.H., 2020. Zinc alleviates cadmium toxicity by modulating photosynthesis, ROS homeostasis, and cation flux kinetics in rice. *Environ. Pollut.* 265, 114979. <https://doi.org/10.1016/j.envpol.2020.114979>.
- An, J.P., Qu, F.J., You, X., Wang, X.F., Hao, Y.J., 2017. Ectopic expression of an apple cytochrome P450 gene MdCYP1 negatively regulates plant photomorphogenesis and stress response in arabidopsis. *Biochem. Biophys. Res. Commun.* 483, 1–9. <https://doi.org/10.1016/j.bbrc.2017.01.026>.
- Anastasiades, M., Lehotay, S.J., Stajnbaher, D., Schenck, F., 2003. Fast and easy multiresidue method employing acetonitrile extraction/partitioning and “dispersive solid-phase extraction” for the determination of pesticide residues in produce. *J. AOAC Int.* 86, 412–431. <https://doi.org/10.1093/jaoac/86.2.412>.
- Arora, S., Mukherjee, I., Kumar, A., Garg, D.K., 2014. Comparative assessment of pesticide residues in grain, soil, and water from IPM and non-IPM trials of basmati rice. *Environ. Monit. Assess.* 186, 361–366. <https://doi.org/10.1007/s10661-013-3380-3>.
- Besse-Hoggan, P., Alekseeva, T., Sancelme, M., Delort, A.M., Forano, C., 2009. Atrazine biodegradation modulated by clays and clay/humic acid complexes. *Environ. Pollut.* 157, 2837–2844. <https://doi.org/10.1016/j.envpol.2009.04.005>.
- Chu, C., Liu, B., Liu, J., He, J., Lv, L., Wang, H., Xie, X., Tao, Q., Chen, Q., 2020. Phytoremediation of acetochlor residue by transgenic arabidopsis expressing the acetochlor N-dealkylase from sphingomonas wittichii DC-6. *Sci. Total Environ.* 728, 138687. <https://doi.org/10.1016/j.scitotenv.2020.138687>.
- Coleman, S., Linderman, R., Hodgson, E., Rose, R.L., 2000. Comparative metabolism of chloroacetamide herbicides and selected metabolites in human and rat liver microsomes. *Environ. Health Perspect.* 108, 1151–1157. <https://doi.org/10.1289/ehp.001081151>.
- Copley, S.D., 2009. Evolution of efficient pathways for degradation of anthropogenic chemicals. *Nat. Chem. Biol.* 5, 559–566. <https://doi.org/10.1038/nchembio.197>.
- Ding, Y., Wang, X., Su, L., Zhai, J.X., Cao, S.Y., Zhang, D.F., Liu, C.Y., Bi, Y.P., Qian, Q., Cheng, Z.K., Chu, C.C., Cao, X.F., 2007. SDG714, a histone H3K9 methyltransferase, is involved in Tos17 DNA methylation and transposition in rice. *Plant Cell* 19, 9–22. <https://doi.org/10.1105/tpc.106.048124>.
- Divi, U.K., Krishna, P., 2009. Brassinosteroid: a biotechnological target for enhancing crop yield and stress tolerance. *New Biotechnol.* 26, 131–136. <https://doi.org/10.1016/j.nbt.2009.07.006>.
- Dixon, D.P., Cummins, I., Cole, D.J., Edwards, R., 1998. Glutathione-mediated detoxification systems in plants. *Curr. Opin. Plant Biol.* 1, 258–266. [https://doi.org/10.1016/S1369-5266\(98\)80114-3](https://doi.org/10.1016/S1369-5266(98)80114-3).
- Feng, S.J., Liu, X.S., Cao, H.W., Yang, Z.M., 2021. Identification of a rice metallochaperone for cadmium tolerance by an epigenetic mechanism and potential use for clean up in wetland. *Environ. Pollut.* 288, 117837. <https://doi.org/10.1016/j.envpol.2021.117837>.
- Feng, S.J., Liu, X.S., Ma, L.Y., Khan, I.U., Rono, J.K., Yang, Z.M., 2020. Identification of epigenetic mechanisms in paddy crop associated with lowering environmentally related

- cadmium risks to food safety. *Environ. Pollut.* 256, 113464. <https://doi.org/10.1016/j.envpol.2019.113464>.
- Huang, M.T., Lu, Y.C., Zhang, S., Luo, F., Yang, H., 2016. Rice (*Oryza sativa*) laccases involved in modification and detoxification of herbicides atrazine and isoproturon residues in plants. *J. Agric. Food Chem.* 64, 6397–6406. <https://doi.org/10.1021/acs.jafc.6b02187>.
- Jiang, Z., Zhang, X., Wang, Z., Cao, B., Deng, S., Bi, M., Zhang, Y., 2019. Enhanced biodegradation of atrazine by arthrobacter sp. DNS10 during co-culture with a phosphorus solubilizing bacteria: enterobacter sp. P1. *Ecotoxicol. Environ. Saf.* 172, 159–166. <https://doi.org/10.1016/j.ecoenv.2019.01.070>.
- Jiao, J., Chen, M., Sun, S., Si, W., Wang, X., Ding, W., Fu, X., Wang, A., Yang, C., 2021. Synthesis, bioactivity evaluation, 3D-QSAR, and molecular docking of novel Pyrazole-4-carbohydrazides as potential fungicides targeting succinate dehydrogenase. *Chin. J. Chem.* 39, 323–329. <https://doi.org/10.1002/cjoc.202000438>.
- Khan, I.U., Rono, J.K., Liu, X.S., Feng, S.J., Li, H., Chen, X., Yang, Z.M., 2020. Functional characterization of a new metallochaperone for reducing cadmium concentration in rice crop. *J. Clean. Prod.* 272, 123152. <https://doi.org/10.1016/j.jclepro.2020.123152>.
- Liu, J.W., Zhang, X., Xu, J.Y., Qiu, J.G., Zhu, J.C., Cao, H., He, J., 2020a. Anaerobic biodegradation of acetochlor by acclimated sludge and its anaerobic catabolic pathway. *Sci. Total Environ.* 748, 141122. <https://doi.org/10.1016/j.scitotenv.2020.141122>.
- Liu, X.S., Feng, S.J., Wang, M.Q., Zhao, Y.N., Cao, H.W., Rono, J.K., Yang, Z.M., 2020b. OsNHAD is a chloroplast membrane-located transporter required for resistance to salt stress in rice (*Oryza sativa*). *Plant Sci.* 291, 110359. <https://doi.org/10.1016/j.plantsci.2019.110359>.
- Li, Y.Y., Yang, H., 2013. Bioaccumulation and degradation of pentachloronitrobenzene in *Medicago sativa*. *J. Environ. Manag.* 119, 143–150. <https://doi.org/10.1016/j.jenvman.2013.02.004>.
- Lu, F.F., Liu, J.T., Zhang, N., Chen, Z.J., Hong, Y., 2020. OsPAL as a key salicylic acid synthetic component is a critical factor involved in mediation of isoproturon degradation in a paddy crop. *J. Clean. Prod.* 262, 121476. <https://doi.org/10.1016/j.jclepro.2020.121476>.
- Lu, Y.C., Luo, F., Pu, Z.J., Zhang, S., Huang, M.T., Yang, H., 2016b. Enhanced detoxification and degradation of herbicide atrazine by a group of O-methyltransferases in rice. *Chemosphere* 165, 487–496. <https://doi.org/10.1016/j.chemosphere.2016.09.025>.
- Lu, Y., Feng, S., Zhang, J., Luo, F., Zhang, S., Yang, H., 2016a. Genome-wide identification of DNA methylation provides insights into the association of gene expression in rice exposed to pesticide atrazine. *Sci. Rep.* 6, 18985. <https://doi.org/10.1038/srep18985>.
- Lu, Y.C., Zhang, S., Miao, S.S., Jiang, C., Huang, M.T., Liu, Y., Yang, H., 2015. Enhanced degradation of herbicide isoproturon in wheat rhizosphere by salicylic acid. *J. Agric. Food Chem.* 63, 92–103. <https://doi.org/10.1021/jf505117j>.
- Ma, L.Y., Zhang, N., Liu, J.T., Zhai, X.Y., Lv, Y., Lu, F.F., Yang, H., 2019. Uptake of atrazine in a paddy crop activates an epigenetic mechanism for degrading the pesticide in plants and environment. *Environ. Int.* 131, 105014. <https://doi.org/10.1016/j.envint.2019.105014>.
- Ma, L.Y., Zhai, X.Y., Qiao, Y.X., Zhang, A.P., Zhang, N., Liu, J., Yang, H., 2021. Identification of a novel function of a component in the jasmonate signaling pathway for intensive pesticide degradation in rice and environment through an epigenetic mechanism. *Environ. Pollut.* 268, 115802. <https://doi.org/10.1016/j.envpol.2020.115802>.
- Ma, L.Y., Zhang, S.H., Zhang, J.J., Zhang, A.P., Li, N., Wang, X.Q., Yu, Q.Q., Yang, H., 2018. Jasmonic acids facilitate the degradation and detoxification of herbicide isoproturon residues in wheat crops (*Triticum aestivum*). *Chem. Res. Toxicol.* 31, 752–761. <https://doi.org/10.1021/acs.chemrestox.8b00100>.
- Pivato, M., Fabrega-Prats, M., Masi, A., 2014. Low-molecular-weight thiols in plants: functional and analytical implications. *Arch. Biochem. Biophys.* 560, 83–99. <https://doi.org/10.1016/j.abb.2014.07.018>.
- Powell, E.R., Faldladdin, N., Rand, A.D., Pelzer, D., Schrunck, E.M., Dhanwada, K.R., 2011. Atrazine exposure leads to altered growth of HepG2 cells. *Toxicol. In Vitro* 25, 644–651. <https://doi.org/10.1016/j.tiv.2011.01.001>.
- Sánchez-Trasviña, C., Enriquez-Ochoa, D., Arellano-Gurrola, C., Tinoco-Valencia, R., Rito-Palomares, M., Serrano-Carreón, L., Mayolo-Deloisa, K., 2019. Strategies based on aqueous two-phase systems for the separation of laccase from protease produced by pleurotus ostreatus. *Fluid Phase Equilib.* 502, 112281. <https://doi.org/10.1016/j.fluid.2019.112281>.
- Scarpato, R., Testi, S., Colosimo, V., Crespo, C.G., Micheli, C., Azzarà, A., Tozzi, M.G., Ghirri, P., 2020. Role of oxidative stress, genome damage and DNA methylation as determinants of pathological conditions in the newborn: an overview from conception to early neonatal stage. *Mutat. Res.* 783, 108295. <https://doi.org/10.1016/j.mrrev.2019.108295>.
- Scialli, A.R., DeSesso, J.M., Breckenridge, C.B., 2014. Developmental toxicity studies with atrazine and its major metabolites in rats and rabbits. *Birth Defects Res. B.* 101, 199–214. <https://doi.org/10.1002/bdrb.21099>.
- Sharma, A., Kumar, V., Kumar, R., Shahzad, B., Thukral, A.K., Bhardwaj, R., 2018. Brassinosteroid-mediated pesticide detoxification in plants: a mini-review. *Cogent Food Agric.* 4, 1436212. <https://doi.org/10.1080/23311932.2018.1436212>.
- Sharma, A., Yuan, H., Kumar, V., Ramakrishnan, M., Kohli, S.K., Kaur, R., Thukral, A.K., Bhardwaj, R., Zheng, B., 2019. Castasterone attenuates insecticide induced phytotoxicity in mustard. *Ecotoxicol. Environ. Saf.* 179, 50–61. <https://doi.org/10.1016/j.ecoenv.2019.03.120>.
- Sharma, A., Thakur, S., Kumar, V., Kesavan, A.K., Thukral, A.K., Bhardwaj, R., 2017. 24-epibrassinolide stimulates imidacloprid detoxification by modulating the gene expression of Brassica juncea L. *BMC Plant Biol.* 17, 56. <https://doi.org/10.1186/s12870-017-1003-9>.
- Siddiqi, K.S., Husen, A., 2021. Significance of brassinosteroids and their derivatives in the development and protection of plants under abiotic stress. *Biologia* 76, 2837–2857. <https://doi.org/10.1007/s11756-021-00853-3>.
- Song, J., Feng, S.J., Chen, J., Zhao, W.T., Yang, Z.M., 2017. A cadmium stress-responsive gene AtFC1 confers plant tolerance to cadmium toxicity. *BMC Plant Biol.* 17, 187. <https://doi.org/10.1186/s12870-017-1141-0>.
- Su, X.X., Zhang, J.J., Liu, J.T., Zhang, N., Ma, L.Y., Lu, F.F., Chen, Z.J., Shi, Z., Si, W.J., Liu, C., Yang, H., 2019. Biodegrading two pesticide residues in paddy plants and the environment

- by a genetically engineered approach. *J. Agric. Food Chem.* 67, 4947–4957. <https://doi.org/10.1021/acs.jafc.8b07251>.
- Sun, J.Y., Liu, X.S., Khan, I.U., Wu, X.C., Yang, Z.M., 2021. OsPIP2;3 as an aquaporin contributes to rice resistance to water deficit but not to salt stress. *Environ. Exp. Bot.* 183, 104342. <https://doi.org/10.1016/j.envexpbot.2020.104342>.
- Sun, X.Y., Zhou, Q.X., Ren, W.J., Li, X.H., Ren, L.P., 2011. Spatial and temporal distribution of acetochlor in sediments and riparian soils of the Songhua River Basin in northeastern China. *J. Environ. Sci.* 23, 1684–1690. [https://doi.org/10.1016/S1001-0742\(10\)60595-5](https://doi.org/10.1016/S1001-0742(10)60595-5).
- Tai, J.K.A., Horzmann, K.A., Franco, J., Jannasch, A.S., Cooper, B.R., Freeman, J.L., 2021. Developmental atrazine exposure in zebrafish produces the same major metabolites as mammals along with altered behavioral outcomes. *Neurotoxicol. Teratol.* 85, 106971. <https://doi.org/10.1016/j.ntt.2021.106971>.
- Tan, L.R., Lu, Y.C., Zhang, J.J., Luo, F., Yang, H., 2015. A collection of cytochrome P450 monooxygenase genes involved in modification and detoxification of herbicide atrazine in rice (*Oryza sativa*) plants. *Ecotoxicol. Environ. Saf.* 119, 25–34. <https://doi.org/10.1016/j.ecoenv.2015.04.035>.
- Taylor, R., 2017. 3.05 -Progress in the understanding of traditional and nontraditional molecular interactions. In: Chackalamanni, S., Rotella, D., Ward, S.E. (Eds.), *Comprehensive Medicinal Chemistry III*. Elsevier, Oxford, pp. 67–100 <https://doi.org/10.1016/B978-0-12-409547-2.12340-6>.
- Wang, Z., Jiang, Y., Peng, X., Xu, S., Zhang, H., Gao, J., Xi, Z., 2017. Exogenous 24-epibrassinolide regulates antioxidant and pesticide detoxification systems in grapevine after chlorothalonil treatment. *Plant Growth Regul.* 81, 455–466. <https://doi.org/10.1007/s10725-016-0223-6>.
- Wirbisky-Hershberger, S.E., Sanchez, O.F., Horzmann, K.A., Thanki, D., Yuan, C.L., Freeman, J.L., 2017. Atrazine exposure decreases the activity of DNMTs, global DNA methylation levels, and dnmt expression. *Food Chem. Toxicol.* 109, 727–734. <https://doi.org/10.1016/j.fct.2017.08.041>.
- Xia, X.J., Zhang, Y., Wu, J.X., Wang, J.T., Zhou, Y.H., Shi, K., Yu, Y.L., Yu, J.Q., 2009. Brassinosteroids promote metabolism of pesticides in cucumber. *J. Agric. Food Chem.* 57, 8406–8413. <https://doi.org/10.1021/jf901915a>.
- Yokota, T., 1999. Chapter 12 - Brassinosteroids. In: Hooykaas, P.J.J., Hall, M.A., Libbenga, K.R. (Eds.), *New Comprehensive Biochemistry*, pp. 277–293 [https://doi.org/10.1016/S0167-7306\(08\)60492-5](https://doi.org/10.1016/S0167-7306(08)60492-5).
- Zhang, J.J., Lu, Y.C., Zhang, S.H., Lu, F.F., Yang, H., 2016. Identification of transcriptome involved in atrazine detoxification and degradation in alfalfa (*Medicago sativa*) exposed to realistic environmental contamination. *Ecotoxicol. Environ. Saf.* 130, 103–112. <https://doi.org/10.1016/j.ecoenv.2016.04.009>.
- Zhang, J.J., Gao, S., Xu, J.Y., Lu, Y.C., Lu, F.F., Ma, L.Y., Su, X.N., Yang, H., 2017. Degrading and phytoextracting atrazine residues in rice (*Oryza sativa*) and growth media intensified by a phase II mechanism modulator. *Environ. Sci. Technol.* 51, 11258–11268. <https://doi.org/10.1021/acs.est.7b02346>.
- Zhang, J.J., Yang, H., 2021. Metabolism and detoxification of pesticides in plants (for review). *Sci. Total Environ.* 790, 148034. <https://doi.org/10.1016/j.scitotenv.2021.148034>.
- Zhou, Y.H., Xia, X.J., Yu, G., Wang, J., Wu, J., Wang, M., Yang, Y., Shi, K., Yu, Y., Chen, Z.G., An, J., Yu, J., 2015. Brassinosteroids play a critical role in the regulation of pesticide metabolism in crop plants. *Sci. Rep.* 5, 9018. <https://doi.org/10.1038/srep09018>.